J Mater Sci (2018) 53:13550–13559

Mechanochemical Synthesis

Kinetics of mechanical activation of Al/CuO thermite

Andrey N. Streletskii[1,4,*], Igor' V. Kolbanev[1], Galina A. Vorobieva[1], Alexander Yu. Dolgoborodov[1,2,3], Vladimir G. Kirilenko[1], and Boris D. Yankovskii[2]

[1] Semenov Institute of Chemical Physics, Russian Academy of Sciences, ul. Kosygina 4, Moscow, Russia 119991
[2] Joint Institute for High Temperatures, Russian Academy of Sciences, Izhorskaya ul. 13/19, Moscow, Russia 125412
[3] National Nuclear Research University MEPhI (Moscow Engineering Physics Institute), Kashirskoe sh. 31, Moscow, Russia 115409
[4] Moscow Institute of Physics and Technology, Institutskii per. 9, Dolgoprudny, Moscow Oblast, Russia 141700

Received: 13 February 2018
Accepted: 5 May 2018
Published online: 4 June 2018

ABSTRACT

The general aspects of the mechanical activation (MA) of Al/CuO thermite compositions based on micron-sized particles and nanopowders of the starting components have been analyzed using X-ray diffraction and hydrogen titration. The latter method has been employed to evaluate the amount of residual oxygen in CuO and Cu_2O from the weight loss during heating in H_2. The reactivity of the activated mixtures was assessed using DSC and TG in combination with mass spectrometric analysis. In addition, we have measured the ignition temperature, burning velocity, and brightness temperature of the reaction products. The results demonstrate that mechanical activation leads to the fragmentation of the components, mixture homogenization, and the formation of a composite, producing "weakly bound" oxygen in CuO_n and causing partial reaction between the components. The total exothermic heat effect in DSC scans, burning velocity, and brightness temperature as functions of specific milling dose (D) have an extremum. The highest reactivity is observed near D = 2 kJ/g, where a sufficient defect density in the components and good mixture homogenization are ensured, but the degree of MA-induced conversion does not exceed 10%. The burning velocity then reaches 400–700 m/s, and the brightness temperature is 3400–3800 °C. The milling dose dependence of the self-ignition temperature has no extremum. The self-ignition temperature steadily decreases with increasing milling dose, even though the ignition knock "power" falls off. The use of nanoparticulate starting components does not appear reasonable.

Introduction

One, relatively new approach to the preparation of fast-burning thermites is preliminary mechanical activation (MA) of micron-sized metal + solid oxidizer powder mixtures in high-energy ball mills [1–6]. The process ensures the fragmentation and intermixing of mixture components at the submicron level and the formation of structural defects, which allows one to raise the rate of the chemical reaction

Address correspondence to E-mail: str@center.chph.ras.ru

https://doi.org/10.1007/s10853-018-2412-3

on the surface of the reactants and, accordingly, to control the energy release. The materials thus produced are referred to as mechanically activated energetic composites (MAECs). A recent review [6] summarized the first data on the formation and properties of defects resulting from the MA of a number of thermite mixtures (MoO_3, $(–CF_2–CF_2–)_n$, Al, Mg). In particular, MA was shown to favor the formation of "weakly bound" oxygen in MoO_3 and considerably reduce the temperature of oxygen release to the gas phase. The process ensures the self-ignition of the thermite at lower temperatures.

This paper focuses on the MA of Al + CuO thermite. This composition offers one of the largest heat effects per unit volume of the mixture (over 20 kJ/cm^3). In addition to the large heat effect, extremely high burning velocities, up to 2500 m/s, were obtained using low-density compositions based on Al + CuO nanopowders (density of charges, ~ 5% of the maximum density) [7]. The ignition and combustion behavior of Al + CuO nanopowder mixtures, including those prepared using MA, has been the subject of rather extensive studies (see, e.g., Refs. [3, 5, 8–12]).

The MA process may involve not only the fragmentation of components, defect generation, and the formation of a composite but also metal–oxidizer chemical interaction processes. In this work, considerable attention is paid to these "parasitic" processes, and optimal mechanical activation conditions are found that maximize the burning velocity and brightness temperature. To quantitatively determine the degree of conversion, the amount of "unutilized" oxygen in CuO_n was evaluated from the weight loss due to the hydrogen reduction of the system. The hydrogen reduction of CuO and Cu_2O has been the subject of systematic studies [13–17].

Materials and methods

As starting materials, we used micron- and nanometer-sized powders: PP-2l Al pyrotechnic powder (flat particles 50–100 × 2–5 μm in dimensions), CuO (analytical grade) ranging in particle size from 20 to 50 μm, V-Alex nanoparticles (100–200 nm), and *n*CuO (50–80 nm) (Advanced Powder Technologies LLC, Tomsk). X-ray diffraction characterization showed that the starting CuO powder consisted of not only CuO but also Cu_2O (25 wt%) and Cu (0.5 wt%).

We prepared powder mixtures with Al/CuO weight ratios of 18.5/81.5 and 19.6/80.4. The theoretical maximum density (TMD) of the former composition is 5.13 g/cm^3.

The mixtures were prepared and activated using two distinct types of ball mills: Aronov vibro mill and Aktivator-2SL planetary mill. The volume of the grinding vials was 108 and 250 mL, the total ball weight was 200 and 300 g, and the powder mixture weight was 15 g in both cases. To prevent overheating of the mixtures, they were milled in 20- to 60-s cycles, with 5- to 10-min breaks. During milling in the Aktivator-2SL, the vials were water-cooled. The total activation time t_a was varied from 1 to 60 min. To eliminate the risk of explosion, the mixtures were milled in an inert atmosphere in the presence of a liquid additive (20–60 mL of hexane).

To compare the degree of MA in different types of activators, use is made of the specific milling dose $D = J \times t_a$ (kJ/g), where J (W/g) is the power intensity of the activator and t_a (s) is the activation time. J can be determined by the method of test objects [18] from the rate at which the specific surface area of a material with known properties increases during milling. In this study, the mixtures were milled in liquid, so the absolute values of D are only approximate, but the relative values of D allow for an objective estimate of the degree of activation in different mills. The estimated power intensity of the Aronov mill is J = 3.7 W/g, and that of the Aktivator-2SL at its full power is J = 9.7 W/g. In what follows, we specify both the activation time and milling dose. The following designations of compositions are used: Al/CuO(v) and Al/CuO(p) are micron-sized components activated in the vibro and planetary mills, respectively, and *n*Al/*n*CuO is nanopowder activated in the planetary mill.

The structure of the MAECs was determined by X-ray diffraction (XRD) on a DRON-3 diffractometer (Cu target X-ray tube). Their reactivity during slow heating (10 °C/min) was assessed by differential scanning calorimetry (DSC) and thermogravimetry (TG) using a simultaneous thermal analysis system (Netzsch STA 449 C Jupiter) in combination with a quadrupole mass spectrometer (QMS 403 C Aelos).

The burning velocity was measured using several experimental implementations. In the case of low-density charges, with porosities from 50 to 75%,

experiments were carried out in metallic, plastic, and glass tubes 5–10 mm in diameter. The charges were ignited by a heated Nichrome wire, spark, or standard electrical pyrotechnic igniter MB-2N (EVF-1).

The burning velocity in the metallic and plastic tubes was measured by detecting the emission from the combustion front using photodiodes with optical fiber. The experimental data were used to determine the average burning velocity 20–200 mm from the ignition site. In the case of the glass tubes, the emission was detected by a Cordin 226-16G high-speed electron-optical camera.

The brightness temperature T_b of the combustion products was measured in the visible range using a four-channel optical pyrometer (effective wavelengths λ = 500, 600, 700, and 800 nm). About 5 g of MAEC powder was poured in portions into a metallic tube 15–20 mm in diameter and densified to a preset density (0.3–0.4 TMD). For ignition, we used either a heated Nichrome wire or a discharge between two electrodes. At the end of the charge, a transparent window and 5-mm-diameter orifice were made. The light from emitting products was directed to the pyrometer by a system of mirrors and optical filters.

The MAEC ignition temperature and delay were determined using a PM-700 muffle furnace. A weighed amount of the powder (30 ± 1 mg) was placed in a container, introduced into a furnace, and dropped on a heated copper plate. The temperature was monitored with an accuracy of 1 °C. The highest temperature was 430 °C. The ignition delay was determined with an accuracy of 1 s using a stopwatch. The operation of the setup was checked using the known ignition temperature of hexogen.

Results and discussion

Optimization of mechanical activation conditions

Figure 1 shows XRD patterns of two samples of a 2Al + CuO (19.6/80.4 wt%) mixture milled for 2 (1) and 20 (2) min.

Both XRD patterns have lines of four phases: Al, CuO, Cu_2O, and Cu. Note that a considerable amount of Cu_2O and trace levels of Cu were already present in the starting CuO. Mechanical activation does not change the phase composition of the system, but the relative intensity of the lines of Cu and Cu_2O increases.

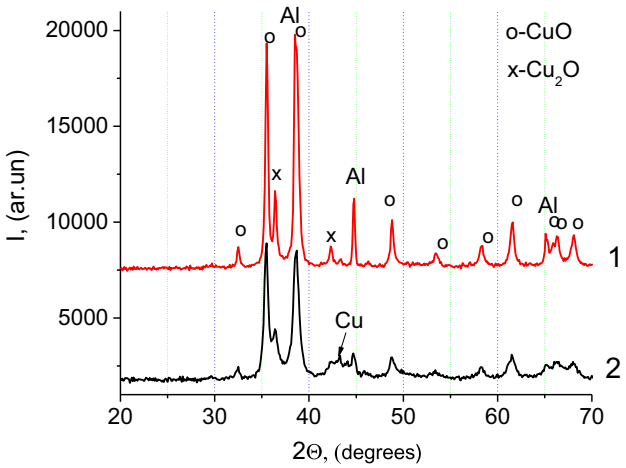

Figure 1 XRD of the Al/CuO(v) mixtures milled for (1) 2 and (2) 20 min. Milling dose D = (1) 0.44 and (2) 4.4 kJ/g.

It is reasonable to assume that milling is accompanied by partial reaction between the mixture components, CuO → Cu_2O → Cu reduction, and the formation of Al_2O_3 as the reaction product. Unfortunately, the forming alumina is X-ray amorphous, so it is inappropriate to use XRD data for assessing the degree of conversion.

To quantify conversion, we determined the concentration of the oxygen persisting in the system in the form of CuO or Cu_2O (remaining unreacted with aluminum). To this end, the milled samples were heated in DSC crucibles under a hydrogen atmosphere. As a result, hydrogen detached oxygen from the copper oxides, resulting in water release to the gas phase, and the sample weight decreased. The constant sample weight at higher temperatures indicated that the copper reduction process reached completion. Curve 1 in Fig. 2 corresponds to the reduction of the unmilled CuO during heating in H_2. It is seen that the weight of the CuO stops decreasing near 550 °C, with $\Delta M/M$ = 18.26%. After reduction, only one phase, Cu, was identified in the sample by XRD, and the weight loss coincided well with the total oxygen content of the initial CuO (~ 17.9 wt%), as can be evaluated from XRD data (see "Materials and methods" section). In further analysis, we assumed that H_2 did not detach oxygen from Al_2O_3 and that the amount of oxygen combined with copper could be estimated in this way.

Curve 2 in Fig. 2 corresponds to the hydrogen reduction of the unmilled Al/CuO mixture. It

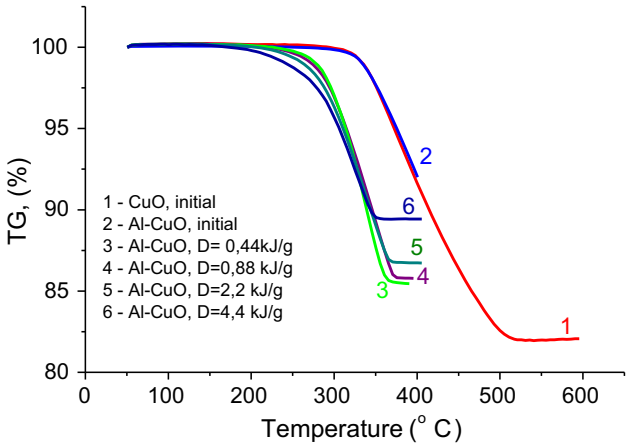

Figure 2 Weight loss of unmilled (1) CuO and (2) Al/CuO and milled (3–6) Al/CuO(v) mixtures during heating in H_2.

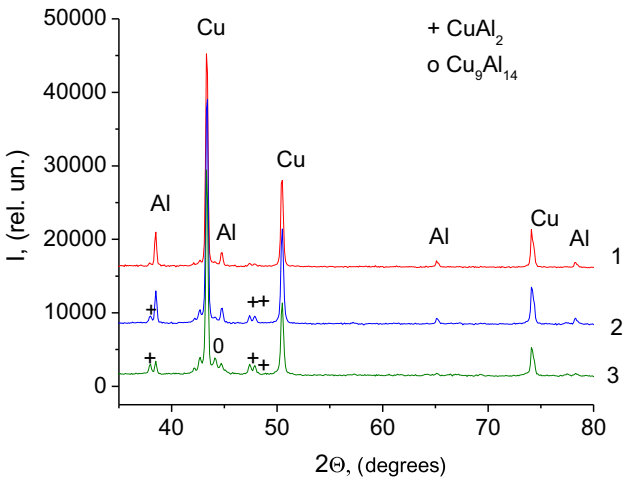

Figure 3 XRD after reduction in H_2 of Al/CuO(v) mixtures. Milling dose D = (1) 0.88, (2) 2.2, and (3) 4.4 kJ/g.

coincides with the curve for the reduction of CuO (curve 1). Curves 3–6 in Fig. 2 correspond to heating of the Al/CuO mixtures in hydrogen after MA to various doses. It is seen that the weight loss curves of the activated mixtures are shifted to lower temperatures by about 70 °C. Further research is needed to find out the nature of the shift of the reduction curves to lower temperatures. It cannot be ruled out that the shift can be understood in terms of the position of Al and Cu in the electrochemical activity series. The electrochemical potential of Al is − 1.7 V, and that of Cu is + 0.522 V [19]. The MA-induced close contact between the mixture components and the resulting potential difference may facilitate hydrogen reduction of the copper oxides.

The XRD data obtained after heating MA mixtures Al/CuO in H_2 (Fig. 3) confirm that the reduction of copper reaches completion. The XRD patterns in Fig. 3 are dominated by lines of Cu and Al. At high milling doses, there are also trace amounts of $CuAl_2$ and Cu_9Al_{14}, without even trace levels of the copper oxides. Thus, gravimetric data on hydrogen reduction can be used to assess the amount of oxygen persisting in CuO_n after MA.

Row 1 in Table 1 summarizes the weight loss data for the samples milled to various doses and then reduced in H_2. The oxygen content of the starting mixture $[O]_{ini}$ was 18.26 × 0.804 = 14.68 wt%. It is seen from row 1 in Table 1 that, for sample with dose D = 0.44 kJ/g, the weight loss due to oxygen detachment equal to 14.58 wt%. With increasing milling dose, the amount of residual oxygen decreases, indicating that the aluminum oxidizes during milling. The data given in row 1 in Table 1 are presented in row 2 as the percentage of oxygen consumed for the oxidation of the aluminum. The fraction of reacted oxygen, $[\Delta O]_R = [O]_{ini} - [O]$, divided by the total amount of oxygen, $[O]_{ini}$, increases from a fraction of a percent at low milling doses to about 10% at doses near 2 kJ/g, reaching ~ 28% at the highest dose. Thus, mechanical activation is accompanied by reaction between the mixture components and, at milling doses above 4 kJ/g, the degree of conversion can reach tens of percent.

Figures 4 and 5 present examples of TG and DSC curves of the unmilled (Fig. 4) and milled (Fig. 5) $(Al/CuO)_v$ mixtures in He. The weight of the starting mixture (Fig. 4, curve 1) decreases by 0.2% in the range ~ 300–400 °C, which is due to CO_2 release. At temperatures above 700–750 °C, we observe further weight loss, due to oxygen release to the gas phase (see curve 5) as a result of the thermal decomposition of CuO. The DSC curve (3) shows endothermic peaks due to aluminum melting and CuO decomposition, accompanied by oxygen release, but there are no well-defined exothermic peaks attributable to aluminum oxidation. During a second heating of the same sample, its weight increases slightly (curve 2), presumably due to the oxidation of the Al by O_2 impurities in He, and the DSC curve shows only the Al melting peak (curve 4), without high-temperature O_2 release (curve 6).

It follows from XRD data that the high-temperature oxygen release is due to the $2CuO \rightarrow Cu_2O + O$

Table 1 The degree of conversion of 2Al + 3CuO reaction ($[\Delta O]_R/[O]_{ini}$) under milling

	t (min)	0	2	4	6	8	10	20
	D (kJ/g)	0	0.44	0.88	1.3	1.8	2.2	4.4
1	wt% [O], (TG-H_2)	–	14.58	14.26	14.03	13.26	13.30	10.61
2	$[\Delta O]_R/[O]_{ini}$ %	0	0.7	2.8	4.4	9.5	9.4	27.7
3	wt% ΔM (> 700 °C) (TG)	− 4.77	− 3.09	− 1.01	− 0.44	0	0	0

t and D are the duration and dose of MA. [O] (TG-H_2) is weight loss in TG measurements during heating in H_2. $[\Delta O]_R/[O]_{ini}$ is the fraction of oxygen that reacted during milling; ΔM (> 700 °C) (TG) is the weight loss due to high-temperature oxygen release

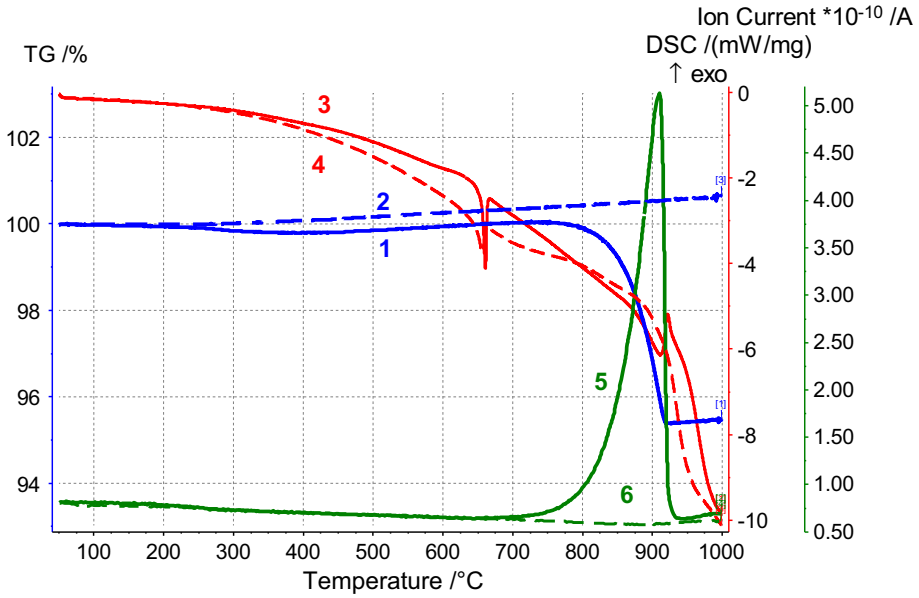

Figure 4 Weight change (1, 2), heat effect (3, 4), and O_2 (m/z = 32) ion currents (5, 6) during first (1, 3, 5) and second (2, 4, 6) heating of the unmilled Al/CuO mixture.

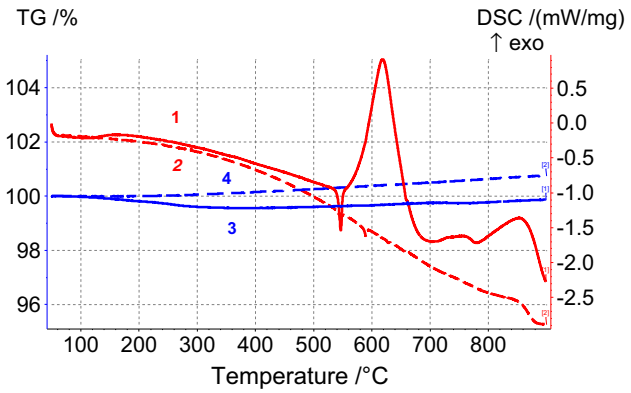

Figure 5 Heat effects (1,2) and weight change (3,4) during the first (1,3) and second (dash) heating of the $(Al/CuO)_v$ MAEC (8 min, D = 1.8 kJ/g).

decomposition and that the only phase present after first heating is Cu_2O. The weight loss due to O_2 release from this sample is 4.77%.

Table 1 (row 3) compares the amounts of oxygen released from different samples to the gas phase above 750 °C (ΔM (> 700 °C)). With increasing milling dose, ΔM (> 700 °C) decreases. Starting at a milling dose of 1.8 kJ/g, we observe no O_2 release to the gas phase. It is reasonable to assume that, at milling doses above 1.8 kJ/g, the mixture is well homogenized and that all of the oxygen released participates in aluminum oxidation reactions.

Figure 5 presents data for the sample milled for 8 min (D = 1.8 kJ/g). The lines 1 and 3 represent the first heating in He, and the lines 2 and 4 represent the second heating. The TG curve 3 shows a weight loss in the range 200–400 °C, due to CO_2 release. At higher temperatures, the sample weight remains essentially unchanged. The formation of CO_2 seems to be due to the thermal decomposition of hexane, which is present in the mixture as a result of the milling in the presence of liquid hexane and is oxidized by oxygen impurities in helium in the calorimeter. The DSC curve 1 shows a small, broad exotherm below 500 °C; an endothermic peak at 540 °C; an exotherm in the range 550–700 °C, overlapping with the aluminum melting endotherm

(660 °C); and two exotherms at 750 and 850 °C. The temperature of the endothermic peak at 540 °C coincides with the eutectic temperature in the Al–Cu system. All of the exothermic peaks correspond to aluminum oxidation. During reheating of the sample, no exotherms were detected, and it DSC curve (2) showed small endotherms at 540, 590, 620, and 650 °C. In this process, the sample weight (curve 4) increases slightly, which seems to be caused by the oxidation of the residual aluminum by trace amounts of oxygen in helium.

The MA of Al/CuO thermite mixtures is known to result in the fragmentation of their components, defect generation, mixture homogenization, and the formation of a composite with a large contact area [3, 5, 6]. It is reasonable to assume that the amount of free high-temperature oxygen (Fig. 4; Table 1, row 3) qualitatively characterizes the degree of homogeneity of the mixtures and the increase in contact area. At temperatures above 750–800 °C and a low oxygen pressure, CuO decomposes to give $Cu_2O + O$ and the oxygen reaches the gas phase. In the case of an unmilled mixture, this oxygen is released in the gas phase (Fig. 4) and does not contribute to the oxidation of aluminum. (O_2 release is an endothermic process.) With increasing milling dose and contact area, the amount of free high-temperature oxygen decreases (Table 1, row 3), and there is no free oxygen at a milling dose of 1.8 kJ/g or above. All of the released high-temperature oxygen reacts with aluminum, and the reaction is exothermic (see the maximum at ~ 850 °C in curve 1 in Fig. 5).

Thus, at a milling dose of 1.8 kJ/g, there is already a rather large contact area between the components, which is capable of "captured" all of the oxygen released.

A negative consequence of the formation of a large contact area is the acceleration of the reaction between the components during milling. At low milling doses, the contact area is small and the degree of milling-induced conversion is insignificant. At milling doses above 1.8 kJ/g, the rate of interaction between the components during milling sharply rises and the degree of conversion caused by mechanical activation approaches almost 30% even at a milling dose of 4.4 kJ/g. Thus, to optimize the mechanical activation of the thermite system, one should stop milling as soon as there is a sufficiently large contact area. The data in Table 1 strongly suggest that optimal milling doses are 1.8–2 kJ/g.

Effect of milling dose on the exothermic heat effect, burning velocity, and brightness temperature

Figure 6 compares the areas of the "main" exothermic peak in the range 550–700 °C at different milling doses. It is seen that the curve has a maximum: the highest heat release is observed after milling for 8–10 min (milling dose of about 2 kJ/g).

The maximum in the heat effect as a function of milling dose is due to the competition between the fragmentation and intermixing of the components on the one hand and partial reaction between them on the other. At low milling doses, the contact area between the components is insufficient, so a considerable part of the oxygen released from CuO during heating escapes to the gas phase without reacting with aluminum. Starting at D = 1.8 kJ/g, all of the oxygen participates in the reaction. At the highest milling dose, a significant degree of conversion is reached in the course of activation in the mill, so the heat effect decreases (Fig. 6).

Table 2 and Fig. 7 present measured burning velocities in porous samples for a number of mixtures.

On the whole, the present burning velocity data demonstrate that mechanical activation to optimal milling doses ensures a considerable increase in burning velocity. In particular, whereas the burning velocity of conventional mixtures does not exceed a few tens of centimeters per second, the low-density MAECs burn with a transition to explosion, leading to the disintegration of thin-walled plastic and

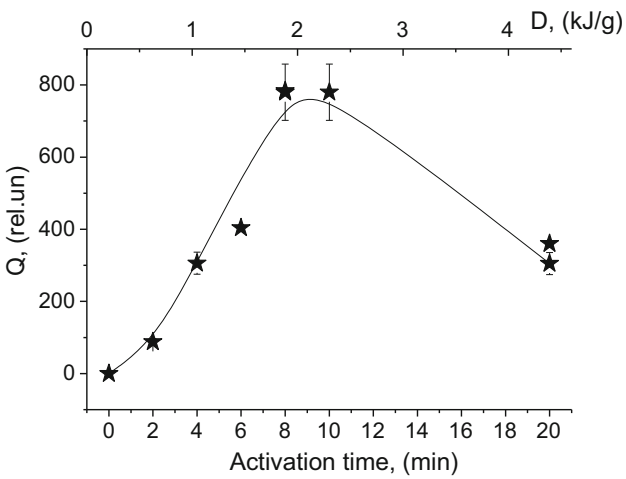

Figure 6 Exothermic heat effect in the range 550–700 °C as a function of milling time (dose D) for $(Al/CuO)_v$.

Table 2 Burning velocity (u) of the mechanically activated mixtures in tubes

Type of mixture	D (kJ/g)	ρ_o (g/cm^3)	ε (%)	Shell	d (mm)	Initiator	L (mm)	u (m/s)
Al/CuO(v)	2.2	1.89	63	Duralumin	10	NiCr	84	120
nAl/nCuO	1.3	1.10	79	Duralumin	10	NiCr	84	82
Al/CuO(v)	2.2	1.54	70	Duralumin	10	NiCr	40	23
Al/CuO(v)	2.2	1.59	69	Duralumin	10	NiCr	57	75
Al/CuO(v)	2.2	1.59	69	Plastic	6.8	NiCr	92	850
Al/CuO(v)	2.2	1.59	69	Copper	6	MB-2 N	129	280
Al/CuO(v)	2.2	1.59	69	Plastic	6.8	MB-2 N	93	670
Al/CuO(v)	2.4	1.55	70	Glass	8	spark	120	105
Al/CuO (p)	0.59	1.80	65	Silicone	6	NiCr	110	240
Al/CuO (p)	1.18	1.70	67	Silicone	6	NiCr	110	340
Al/CuO (p)	1.77	1.60	69	Silicone	6	NiCr	110	460
Al/CuO (p)	2.36	1.80	65	Silicone	6	NiCr	110	110

D milling dose, ρ_o density of the mixture, ε porosity, d diameter, L distance from the ignition site

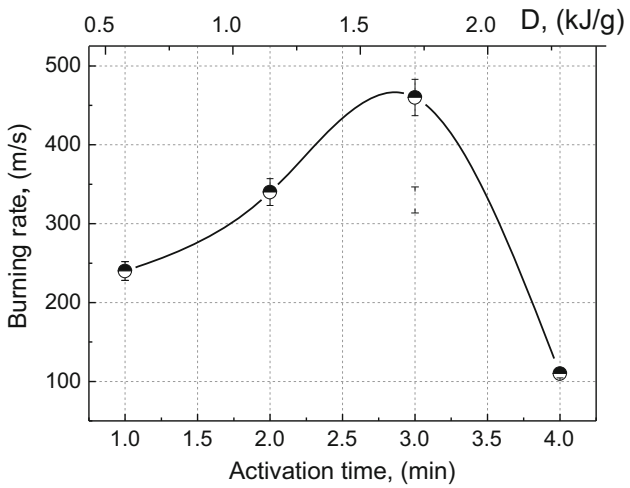

Figure 7 Burning velocity as a function of milling time (dose) for $(Al/CuO)_p$.

metallic shells. Burning velocity depends on the particle size and shape of the starting components, the density of the mixture, and the milling dose.

The highest burning velocities were obtained for the Al/CuO(v) and Al/CuO(p) mixtures at a relative density near 0.3. The burning velocity of the MAECs depends to a significant degree on the shell material and diameter, the ignition technique, and the distance between the ignition and velocity measurement sites. In most experiments, combustion was initiated by pulsed heating (30–50 ms) of a Nichrome wire (2.8–3 Ω). The process accelerates from slow burning with velocities at a level of 10 m/s to fast burning at 400–700 m/s.

Figure 8 shows the measured brightness temperature T_b of the combustion products of different MAECs. T_b varies from 2500 to 3800°K, depending on the MAEC composition and milling conditions. The highest T_b (up to 3800°K) was obtained for Al/CuO(p) at D near 2 kJ/g. Further increasing D leads to a decrease in T_b. The brightness temperatures of all the mixtures studied here vary strongly with wavelength (by up to 400°K), which can be interpreted as evidence that the state of the reaction products is significantly displaced from equilibrium.

Thus, despite the slight distinctions, on the whole the burning velocity and brightness temperature data are consistent with the DSC + TG data, which

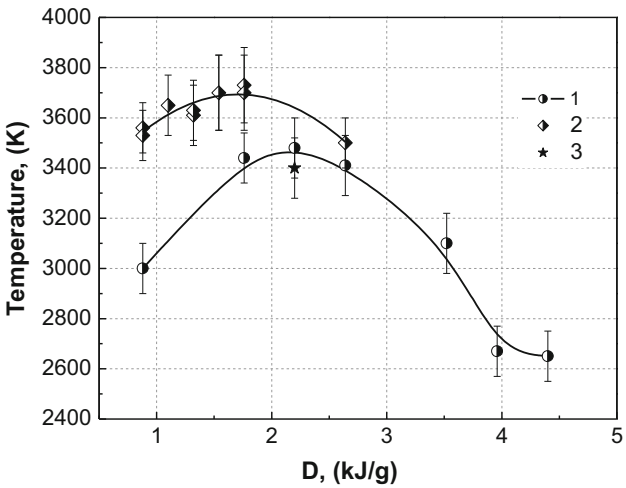

Figure 8 Brightness temperature as a function of milling dose D for (1) Al/CuO(v), (2) Al/CuO(p), and (3) nAl/nCuO.

indicate that the highest reactivity is offered by the pyrotechnic powder-based MAEC at a milling dose of about 1.8–2.2 kJ/g.

Effect of milling dose on the ignition delay and the role of "weakly bound" oxygen

Figure 9 shows the self-ignition delay of the activated composites in contact with a hot surface maintained at temperature T. Line 1 refers to the Al/CuO(v) MAEC, with an initial particle size in the micron range, after milling to D = 2.2 kJ/g. The temperature 340 °C corresponds to the lowest temperature at which self-ignition occurred in ~ 1 s. The arrows indicate temperatures at which no self-ignition occurred. The lowest temperature at which self-ignition was detected in run 1 in Fig. 9 is 263 °C.

Table 3 illustrates the effect of milling dose on the lowest thermite self-ignition temperature. It is seen that, at a low milling dose, no self-ignition was detected, because the self-ignition temperature exceeded the highest substrate temperature (430 °C).

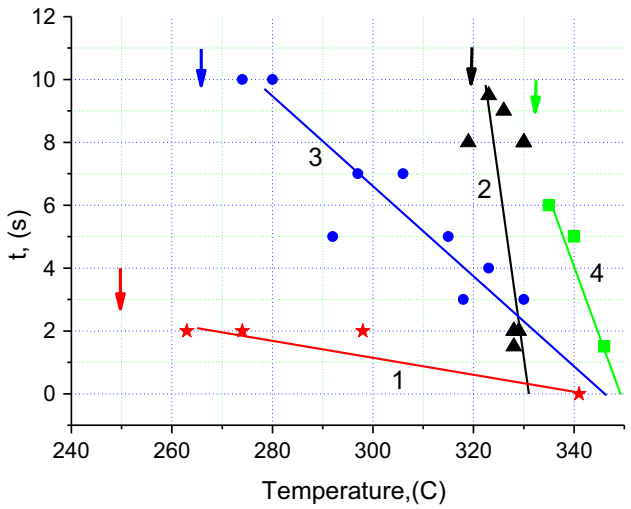

Figure 9 Ignition delay t as a function of substrate temperature for the MAECs. Mechanical activation of (1) micron-sized particles and (2–4) nanoparticulate components. Milling doses of (1) 2.2, (2) 1.5, (3) 2.9, and (4) 4.3 kJ/g.

Table 3 Minimum ignition temperatures T_{ign} of the Al/CuO(v) MAEC in contact with a hot surface

t (min)	2	4	6	8	10	12	20
D (kJ/g)	0.44	0.88	1.3	1.8	2.2	3.1	4.4
T_{ign} (°C)	> 430	> 430	> 430	333	263	250	175

t time, D milling dose

At the optimal milling dose (2.2 kJ/g), the lowest self-ignition temperature is 263 °C (as seen from line 1 in Fig. 9). At higher milling doses (3.1 and 4.4 kJ/g), however, self-ignition occurs at noticeably lower temperatures (down to 175 °C), but the self-ignition knock intensity decreases.

To shed light on the last series of experiments, Table 4 shows the measured amount of residual oxygen bonded to copper after heating in an inert atmosphere to different temperatures. Before this, the sample was reheated in a hydrogen atmosphere after the first heating in He. The last column in Table 4 indicates the amount of "weakly bound" oxygen, M1, which enters into the reaction below 500 °C, for two samples (with the optimal and maximal milling doses). It is seen that, with increasing milling dose, the amount of "weakly bound" oxygen persisting in the material after milling rises even though the degree of conversion also increases with milling dose.

Another piece of evidence that, with increasing milling dose, the amount of the most "weakly bound" oxygen in the sample increases, in spite of the reaction occurring in the system, is the systematic shift of the onset of reduction in hydrogen to lower temperatures, as seen from curves 3–6 in Fig. 2.

Thus, the optimal milling dose maximizes the heat of the reaction, burning velocity, and brightness temperature. At the same time, a small amount of "weakly bound" oxygen is responsible for self-ignition. Raising the milling dose increases the amount of oxygen in the "weakly bound" state.

Experiments with nanoparticulate starting components

We carried out several experiments aimed at activating a mixture of nanopowders [nCuO + nAl (Alex)]. Comparison of Figs. 10 and 5 demonstrates that, after mechanical activation of the nanopowders, interaction is observed at higher temperatures in comparison with the mixtures of the micron-sized particles. In the former case, there are two sharp exothermic peaks at temperatures higher than 590 and 660 °C, which correspond to the melting points of the intermetallic phase $CuAl_2$ and Al. Thus, in the case of the nanoparticulate starting components, transformations accompanied by heat release begin only upon liquid phase formation. The brightness temperature (Fig. 8, data point 3) and burning velocity (Table 2) of the nAl/nCuO composites are

Table 4 Weight loss during reduction in H_2 after preheating in He to different temperatures

Heating in He	50 °C	500 °C	700 °C	$M_1 = M(50)–M(500)$
8 min (1.8 kJ/g)	13.28	12.44	7.16	0.84 (13.28–12.44)
20 min(4.4 kJ/g)	10.61	8.98		1.63 (10.61–8.98)

Al/CuO(v) sample with the optimal (8 min) and highest (20 min) milling times

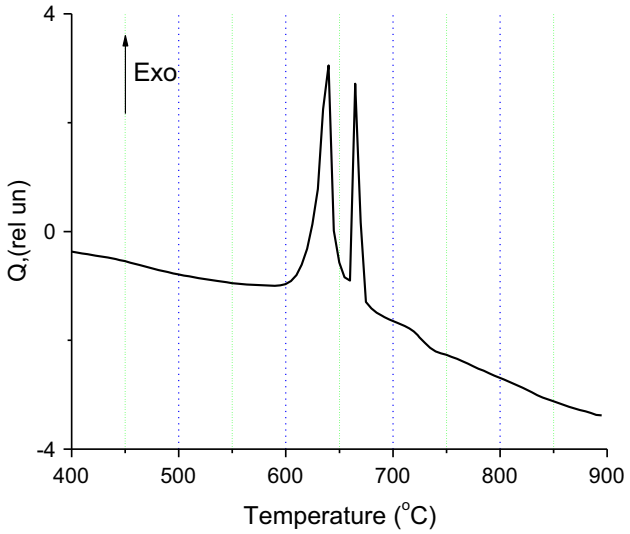

Figure 10 DSC curves of an activated nAl + nCuO nanopowder mixture.

similar to or lower than those of the composites prepared using micron-sized particles. Self-ignition experiments with activated nAl/nCuO mixtures in contact with a hot substrate (Fig. 9, curves 2–4) also showed that these compositions did not have any advantages. In those experiments, a large scatter in the data was observed, there was no clear correlation with the milling dose, and the self-ignition temperature always exceeded that of the mixtures prepared using micron-sized particles. Thus, the use of nanopowders as starting components offers no significant advantages.

Conclusions

The MA of Al/CuO thermite mixtures at room temperature is accompanied by not only the fragmentation of their components, defect generation, mixture homogenization, and formation of dense composites but also chemical reaction between the mixture components. In the range of milling doses studied, the degree of milling-induced conversion can reach almost 30%. The formation of dense composites can be qualitatively characterized by the amount of oxygen released during high-temperature (750–850 °C) CuO decomposition to Cu_2O. Optimal MA conditions are determined on the one hand by the condition that the contact between the mixture components be as close as possible, so that all of the oxygen released from the CuO reacts with the aluminum, and on the other hand by the condition that the consumption of the components in the "parasitic" reaction during milling be minimized. Under the conditions of our experiments, the optimal milling dose is 1.8–2 kJ/g. These milling doses ensure the maximum heat release, burning velocity, and brightness temperature, even though these parameters have slightly different dependences on the milling dose.

As shown earlier [6], the mechanical activation of oxides, including MoO_3, is accompanied by the formation of "weakly bound" oxygen, leading to a low-temperature oxygen release. The process initiates self-ignition of thermite mixtures at low temperatures. In this study, we have obtained the first indirect evidence for the formation of "weakly bound" oxygen in CuO during the activation of an Al/CuO thermite mixture. We have detected a low-temperature exothermic peak below 500 °C. That reaction with aluminum occurs at these temperatures is also evidenced by a chemical method: hydrogen reduction. The amount of "weakly bound" oxygen, capable of reacting during heating below 500 °C, increases with milling dose, even though there is active chemical interaction during milling. Thus, as a result of the reaction, more and more oxygen becomes "weakly bound." Finally, the fact that, when a sample is brought into contact with a hot substrate, the self-ignition temperature decreases with increasing milling dose without extrema also seems to be due to the accumulation of "weakly bound" oxygen. It is worth noting that another possible cause of the increased reactivity of the oxygen in CuO when there is a close contact between the Al and CuO is the difference in electrochemical potential between Al and Cu. Further research is needed to separately assess the contributions of the two mechanisms in question.

The first experiments on the MA of composites with the use of nanoparticulate starting components show that this approach offers no additional possibilities of accelerating the process and does not appear reasonable.

Acknowledgements

This work was financially support by FASO of Russia (ICP RAS—A. N. Streletskii, I. V. Kolbanev, G. A. Vorobieva, V. G. Kirilenko—Project 0082-2018-002, Registration Code AAAA-A18-118031490034-6, and JIHT RAS—A. Yu. Dolgoborodov, B. D. Yankovskii—Project 0044-2014-0016, Registration Code AAAA-A16-116051810082-7). The authors are grateful to A. V. Leonov for XRD measurements.

Compliance with ethical standards

Conflict of interest The authors declare that they have no conflict of interest.

References

[1] Dolgoborodov AYu, Makhov MN, Kolbanev IV, Streletskii AN (2004) Mechanically activated pyrotechnic composition, RF patent no. 2235085, Buyl. Izobr. no. 24

[2] Dreizin EL, Schoenitz M (2009) Nano-composite energetic powders prepared by arrested reactive milling, US patent no. 7,524,355 B2

[3] Dreizin EL (2009) Metal-based reactive nanomaterials. Prog Energy Combust Sci 35:141–167

[4] Dolgoborodov AYu (2015) Mechanically activated oxidizer-fuel energetic composites. Combust Explos Shock Waves 51(1):86–99

[5] Dreizin EL, Schoenitz M (2017) Mechanochemically prepared reactive and energetic materials: a review. J Mater Sci 52(20):11789–11809. https://doi.org/10.1007/s10853-017-0912-1

[6] Streletskii AN, Sivak MV, Dolgoborodov AYu (2017) Nature of high reactivity of metal/solid oxidizer nanocomposites prepared by mechanoactivation: a review. J Mater Sci 52(20):11810–11825. https://doi.org/10.1007/s10853-017-1277-1

[7] Thiruvengadathan R, Bezmelnitsyn A, Apperson S, Staley C, Redner P, Balas W, Nicolich S, Kapoor D, Gangopadhyay K, Gangopadhyay S (2011) Combustion characteristics of novel hybrid nanoenergetic formulations. Combust Flame 158(5):964–978

[8] Zachariah MR, Egan GC (2016) Mechanisms and microphysics of energy release pathways in nanoenergetic materials. In: Zarko V (eds) Energetic nanomaterials: synthesis, characterization, and application. Elsevier, New York City, pp 65–94

[9] Ermoline A, Schoenitz M, Dreizin EL (2011) Reaction leading to ignition in fully dense nanocomposite Al-oxide systems. Combust Flame 158:1076–1083

[10] Ermoline A, Stamatis D, Dreizin EL (2012) Low temperature exothermic reaction in fully dense Al–CuO nanocomposite powders. Thermochim Acta 527:52–58

[11] Baijot V, Mehdi D-R, Rossi C, Esteve A (2017) A multiphase micro-kinetic model for simulating aluminum based thermite reactions. Combust Flame 180:10–19

[12] DeLisio JB, Yi F, LaVan DA, Zachariah MR (2017) High heating rate reaction dynamics of Al/CuO nanolaminates by nanocalorimetry-coupled time of flight mass spectrometry. J Phys Chem C 121:2771–2777

[13] Poulston S, Parlett PM, Stone P, Bowker M (1996) Surface oxidation and reduction of CuO and Cu_2O studied using XPS and XAES. Surf Interface Anal 24:811–820

[14] Kim JY, Rodrigues JA, Hanson JC, Frenkel AI, Lee PL (2003) Reduction of CuO and Cu_2O with H_2: H embedding and kinetic effects in the formation of suboxides. J Am Chem Soc 125:10684–10692

[15] Rodriguez JA, Kim JY, Hanson JC, Perez M, Frenkel AI (2003) Reduction of CuO in H_2: in situ time-resolved XRD studies. Catal Lett 85:247–254

[16] Kirsch PD, Ekerdt JG (2001) Chemical and thermal reduction of thin film of copper(II) oxide and copper(I) oxide. J Appl Phys 90:4256–4264

[17] Firmansyah DA, Kim T, Kim S, Sullivan K, Zachariah MR, Lee D (2009) Crystalline phase reduction of cuprous oxide (Cu_2O) nanoparticles accompanied by a morphology change during ethanol-assisted spray pyrolysis. Langmuir 25:7063–7071

[18] Streletskii AN (1993) Measurements and calculation of main parameters of power mechanical treatment in different mills. In: de Barbadillo JJ, Froes FH, Schwarz R (eds) Proceedings of the 2nd international conference on structural application of mechanical alloying, Vancouver, Canada, 20–22 September 1993. ASM International, Materials Park, pp 51–58

[19] Vanysek P (2000) Electrochemical series/handbook of chemistry and physic, 81th edn. CRC Press. LLC. ISBN978-0849304811